

The Cellular Autophagy Pathway Modulates Human T-Cell Leukemia Virus Type 1 Replication

Sai-Wen Tang, Chia-Yen Chen, Zachary Klase, Linda Zane, Kuan-Teh Jeang

Molecular Virology Section, Laboratory of Molecular Microbiology, National Institute of Allergy and Infectious Diseases, National Institutes of Health, Bethesda, Maryland, USA

Autophagy, a general homeostatic process for degradation of cytosolic proteins or organelles, has been reported to modulate the replication of many viruses. The role of autophagy in human T-cell leukemia virus type 1 (HTLV-1) replication has, however, been uncharacterized. Here, we report that HTLV-1 infection increases the accumulation of autophagosomes and that this accumulation increases HTLV-1 production. We found that the HTLV-1 Tax protein increases cellular autophagosome accumulation by acting to block the fusion of autophagosomes to lysosomes, preventing the degradation of the former by the latter. Interestingly, the inhibition of cellular autophagosome-lysosome fusion using bafilomycin A increased the stability of the Tax protein, suggesting that cellular degradation of Tax occurs in part through autophagy. Our current findings indicate that by interrupting the cell's autophagic process, Tax exerts a positive feedback on its own stability.

Human T-cell leukemia virus type 1 (HTLV-1), a member of the deltaretrovirus family, is the first identified human retrovirus (1, 2). HTLV-1 infects an estimated 15 to 20 million individuals worldwide (3, 4). HTLV-1 predominantly infects CD4⁺ lymphocytes and is primarily transmitted through cell-to-cell contact; free virions do not efficiently infect cells (5, 6). Infection by HTLV-1 causes adult T-cell leukemia (ATL) (2, 7–9) and a neurodegenerative disease, HTLV-1-associated myelopathy/tropical spastic paraparesis (HAM/TSP) (10, 11). The HTLV-1 regulatory protein Tax is an oncoprotein that plays an essential transcriptional role in viral replication and is involved in virus-mediated transformation of T lymphocytes (11–15). Tax activates the HTLV-1 5' long terminal repeat (LTR) through interaction with transcription factors ATF/CREB (activating transcription factor/cyclic AMP response element binding protein) (16–21). In addition, Tax is able to transactivate or transrepress more than 100 cellular genes through binding and modulating the stability and activity of various cellular proteins (22–27).

Autophagy is a lysosomal degradation pathway used for the removal of misfolded or aggregated proteins and damaged organelles (28, 29). Under nutrient-stressed conditions, autophagy is activated to degrade proteins in order to produce a limited amount of nutrients for cell survival. During the process of autophagy, membrane entities called phagophores are formed; they fuse to form enclosed double-membrane vesicles, known as autophagosomes, that sequester cytoplasmic material. Upon autophagy induction, a processed LC3-II (lipidated Atg8/LC3) protein is generated from its precursor, LC3-I, by conjugation with phosphatidylethanolamine (PE). LC3-II is specifically localized in autophagosomes and is commonly employed as a well-characterized autophagosome marker (30). In a late step of autophagy, matured autophagosomes merge with lysosomes to form autolysosomes, whose contents, including the LC3-II protein, are degraded by the acidic lysosomal enzymes (31, 32).

Besides its role in supporting cellular metabolism in nutritionally stressed settings, autophagy can serve an innate immunity role protecting cells by removing invading intracellular microbial pathogens, such as viruses and bacteria (33, 34). Many viruses have evolved mechanisms to usurp the cell's autophagic degradation defense, adapting this pathway instead to enhance viral rep-

lication (35). For example, herpes simplex virus 1 (HSV-1) is able to suppress the host's autophagy response, and in macrophage infection, the formation of the autophagosome is enhanced for major histocompatibility complex (MHC) class I presentation of viral antigens (36, 37). Nevertheless, the overall role of autophagy in HSV-1 replication remains unclear (36), with other reports demonstrating that in different contexts, autophagy inhibits viral pathogenesis (35). Similarly, influenza A virus infection also triggers autophagosome accumulation. Here, the process appears to be mediated by the viral M2 protein that acts to block the fusion of autophagosomes with lysosomes, preventing the degradation of autophagosomes and leading to their accumulation (38). Nonetheless, to date, the outcome of this process is not well understood because accumulated autophagosomes seem to have no significant effect on viral replication (35). Finally, in the case of retroviruses, human immunodeficiency virus type 1 (HIV-1) has been described to cause the accumulation of autophagic vacuoles in macrophages (39–41), but the effect of HIV-1 infection on autophagy in CD4⁺ T cells is still controversial (40, 42, 43). It has been reported that secreted HIV-1 Tat protein can suppress the autophagy process induced by gamma interferon (IFN- γ) or rapamycin in bystander uninfected macrophages (44, 45). In HIV-1-infected macrophages, the HIV-1 Nef protein has been implicated in blocking the fusion of autophagosomes with lysosomes (41), and there is also suggestive evidence that autophagy might serve to enhance HIV-1 replication (41, 46, 47). In a recent review, it was suggested that Tax may increase autophagy through NF- κ B activation (48), and recent data have shown that HTLV-2 Tax can increase autophagic activity in immortalized CD4⁺ T cells (49).

Here, we demonstrate that HTLV-1 infection accumulates

Received 13 August 2012 Accepted 14 November 2012

Published ahead of print 21 November 2012

Address correspondence to Kuan-Teh Jeang, kjeang@nih.gov.

Supplemental material for this article may be found at <http://dx.doi.org/10.1128/JVI.02147-12>.

Copyright © 2013, American Society for Microbiology. All Rights Reserved.

doi:10.1128/JVI.02147-12

autophagosomes and that this accumulation benefits virus replication. We find that the HTLV-1 Tax protein induces the accumulation of autophagosomes by blocking the fusion of autophagosomes with lysosomes through an NF- κ B-dependent pathway.

MATERIALS AND METHODS

Cells and transfection. HeLa and 293T cells were maintained in Dulbecco's modified Eagle's medium (DMEM) supplemented with 10% fetal bovine serum (FBS), 2 mM/liter L-glutamine, and antibiotics in 5% CO₂ at 37°C. MT2 and Jurkat T cells were maintained in RPMI 1640 with 10% FBS, 2 mM/liter L-glutamine, and antibiotics. To obtain starvation conditions, cells were washed three times with phosphate-buffered saline (PBS) and incubated in Earle's balanced salt solution (EBSS) at 37°C for 3 h. HeLa and 293T cells were transfected using Lipofectamine Plus reagent (Invitrogen) according to the manufacturer's protocols. MT2 and Jurkat T cells were transfected using the Nucleofector kit V (Amaxa Biosystems) following the manufacturer's instructions.

Plasmids and stable cell lines with HTLV-1 LTR-GFP reporter. HTLV-1 LTR-green fluorescent protein (GFP) reporter plasmid was constructed by inserting the XmaI-XhoI fragment of the HTLV-1 LTR from HTLV-1 molecular clone pACH into the pAcGFP1-1 promoterless vector, which contains a neomycin resistance gene (Clontech). To generate cells with integrated HTLV-1 LTR-GFP reporter, HeLa cells were transfected the HTLV-1 LTR-GFP reporter plasmid that was constructed as described above; the transfectants were then selected by G418 for 14 days. The Cherry-LC3 plasmid was a gift from Terje Johansen (50). The HTLV-1 k30 molecular clone was obtained from the NIH AIDS Research and Reference Reagent Program (51). The red fluorescent protein (RFP)-GFP-LC3 plasmid was kindly shared by Tamotsu Yoshimori (52, 53). pEGFP-Tax, pCAG-Flag-Tax, pCAG-Flag-M22, and pCAG-Flag-M47 were previously described (54). The Tax V89A mutant was a gift from Chou-Zen Giam.

Antibodies and reagents. Anti-LC3B antibody was purchased from Novus Biologicals. Antiactin was from Millipore. Antitubulin, anti-Flag, and EBSS were obtained from Sigma-Aldrich. Anti-Tax was from the NIH AIDS Research and Reference Reagent Program. Bafilomycin A (BFA), chloroquine (CQ), MG132, and Hoechst dye were from Sigma-Aldrich. The HTLV-1 p19 enzyme-linked immunosorbent assay (ELISA) kit and anti-p19 antibody were from Zeptomatrix. Lamp2-specific small interfering RNA (siRNA) (M-011715-00) and nontargeting siRNA (D-001206-13) were obtained as siGENOME SMARTpool reagents from Dharmacon.

Ex vivo infection of cells with HTLV-1. For HTLV-1 infection of HeLa cells, 5×10^4 cells were cocultured with MT2 cells at ratios of 1:0, 1:0.5, 1:1, and 1:2 in RPMI 1640 with 10% FBS, 2 mM/liter L-glutamine, and antibiotics, or as a control, the same number of cells was cocultured with Jurkat cells at a ratio of 1:1 for 3 days. After 3 days, the cells were washed with PBS three times to remove the MT2 or Jurkat cells; the washed adherent HeLa cells were then lysed for Western blotting or fixed by 4% paraformaldehyde in PBS for confocal microscopy analysis. For HTLV-1 infection of primary peripheral blood mononuclear cells (PBMCs), PBMCs were enriched from donor blood using Ficoll density gradient separation, and 1×10^6 cells were cocultured with lethally γ -irradiated (60 Gy) MT2 cells at a ratio of 5:1 in RPMI 1640 with 10% FBS, 2 mM/liter L-glutamine, and antibiotics in the presence of 100 U/ml of recombinant interleukin-2 for 14 days as described previously (55).

Immunofluorescence and confocal microscopy. Transfected cells were washed twice with PBS and fixed in 4% paraformaldehyde in PBS for 15 min. For immunofluorescence staining of Flag-Tax protein, cells were permeabilized with 0.2% Triton X-100, blocked with 1% bovine serum albumin (BSA), and then stained by anti-Flag antibody, followed by Alexa 647-conjugated secondary antibody (Invitrogen). DNA was counterstained with Hoechst 33342 (Sigma-Aldrich). Coverslips were mounted in ProLong Gold antifade reagent (Invitrogen), and fluorescence signals were visualized with a Leica TCS SP5 microscope.

Western blotting. The cells were washed with PBS twice and then lysed in lysis buffer (50 mM Tris-HCl [pH 7.5], 150 mM NaCl, 5 mM EDTA, 1% Triton X-100, 0.1% SDS) supplemented with protease inhibitor cocktail (Roche). The lysates were resolved by 12% SDS-PAGE and transferred to polyvinylidene fluoride membranes (Millipore). The membrane was incubated with primary antibodies, followed by alkaline phosphatase-conjugated secondary antibodies (Sigma-Aldrich). Signals were visualized using chemiluminescence following the manufacturer's protocol (Chemicon). Band intensities were quantified using the ImageJ software (56). Loading controls were either tubulin or actin protein. Because Tax and actin migrate in very close proximity on the gel, whenever actin was used in Western blotting, the same loading was repeated on a second gel to make a duplicate Western blot.

RESULTS

HTLV-1 infection induced autophagosome accumulation. To investigate the effect of HTLV-1 on the autophagy pathway, HeLa cells were cotransfected with HTLV-1 LTR-GFP and Cherry-LC3 (50) plasmid. The transfected cells were mock cocultured or cocultured with HTLV-1-producing MT2 cells for 3 days, allowing the latter to infect the former cells. LC3 is a constituent marker of autophagosomes. We compared the mock-cocultured cells to MT2-cocultured cells, examining them for the accumulation of punctated signals of Cherry-LC3 that mark the autophagosomes (Fig. 1A). MT2-cocultured HeLa cells, compared to mock-cocultured cells, indeed showed significantly higher accumulations of fluorescent autophagosomes (white arrows in Fig. 1A).

We repeated the above analysis in Jurkat cells (Fig. 1B). Similar to what was seen with HeLa cells, MT2-mediated HTLV-1 infection of Jurkat cells also significantly increased the accumulation of Cherry-LC3-autophagosomes compared to the level in control Jurkat cells (Fig. 1B). The accumulation of autophagosomes by HTLV-1 infection was further checked by Western blotting of endogenous LC3-II (lipidated Atg8/LC3) in HeLa cells. Indeed, consistent with the accumulation of Cherry-LC3-autophagosomes, the amount of LC3-II (14 kDa) increased in a dose-dependent fashion with the amount of MT2 cells used to mediate HTLV-1 infection of HeLa cells (Fig. 1C, lanes 2 to 4). As a control, coculture of HeLa cells with Jurkat T cells, which are uninfected and produce no HTLV-1, did not increase LC3-II (Fig. 1C, lane 5). Moreover, we addressed this issue by coculturing lethally irradiated MT-2 cells with primary human peripheral blood mononuclear cells (PBMCs) for 14 days (Fig. 1D). The lethally irradiated MT-2 cells after 14 days in culture were fully disintegrated and produced no LC3-II or actin signal by Western blotting (Fig. 1D, lane 3). On the other hand, coculturing for 14 days of the same lethally irradiated MT-2 cells with primary PBMCs increased LC3-II in the latter, compared to culturing of the PBMCs alone, as quantified by Western blotting (Fig. 1D, compare lane 2 to lane 1). This result supports the interpretation that MT2-mediated HTLV-1 infection of PBMCs increases autophagosome accumulation. Taken together, the data in Fig. 1 are consistent with HTLV-1 infection increasing autophagosomes in HeLa cells, Jurkat cells, and human primary PBMCs.

Increased autophagosome accumulation correlated with enhanced HTLV-1 production. We next asked how increased cellular autophagosomes impact HTLV-1 replication. To address this question, we transfected 293T cells with the HTLV-1 k30 molecular clone (51). The transfected cells were then treated with various concentrations (2 to 50 nM) of bafilomycin A (BFA) for 24 h. BFA is a specific inhibitor of vacuolar proton ATPase, whose in-

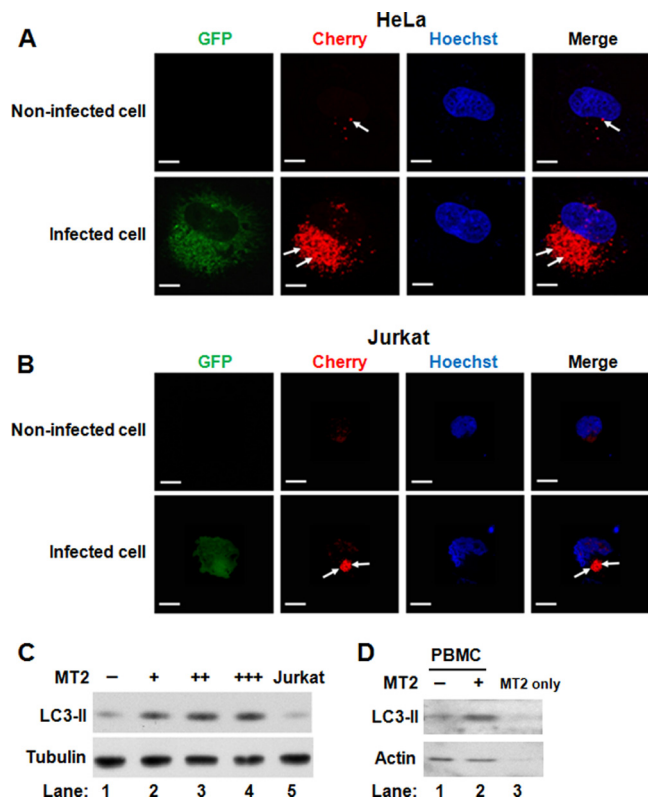


FIG 1 HTLV-1 infection induced the accumulation of autophagosomes. HeLa (A) or (B) Jurkat cells were transfected with HTLV-1 LTR-GFP and Cherry-LC3 plasmids and then cocultured with or without MT2 cells for 3 days at ratios of 1:1 (HeLa/MT2) or 5:1 (Jurkat/MT2), respectively. Fluorescent signals were detected by confocal microscopy. The arrows point to fluorescent puncta of Cherry-LC3, green shows GFP signal, and blue shows nuclear Hoechst staining. Bars, 10 μ m. (C) HeLa cells were cocultured with MT2 cells at a ratio of 1:0 (–) (lane 1), 1:0.5 (+) (lane 2), 1:1 (++) (lane 3), and 1:2 (+++) (lane 4) or with Jurkat cells at a ratio of 1:1 (Jurkat) (lane 5) for 3 days. Afterwards, the cells were washed with PBS three times to remove the MT2 or Jurkat cells; the washed HeLa cells were then lysed, and the lysates were Western blotted with anti-LC3B (LC3-II; 14 kDa) and antitubulin (Tubulin) antibodies. Tubulin was used as a loading control. (D) PBMCs were cocultured with irradiated MT2 (lane 2) cells at a ratio of 5:1 for 14 days as described in Materials and Methods. PBMC-only (lane 1) and irradiated MT2-only (lane 3) cultures are controls. The lysates were Western blotted with anti-LC3B (LC3-II) and antiactin (Actin) antibodies. Actin was used as a loading control.

hibition is known to block the fusion of autophagosomes with lysosomes; thus, BFA treatment leads to the accumulation of autophagosomes (57). Mock-treated and BFA-treated cells were then compared for HTLV-1 production by measuring the amount of viral capsid protein in the cell culture supernatant using p19 ELISA. BFA treatment indeed increased autophagosome accumulation, as evidenced by Western blotting for LC3-II protein (Fig. 2A, bottom), and BFA treatment also produced a dose-dependent increase in HTLV-1 particle production, as measured by p19 in the culture supernatant (Fig. 2A, bar graph, top). Chloroquine (CQ) is also able to prevent the autophagosome-lysosome fusion by elevating the pH of lysosomes (58, 59), and we observed that CQ treatment similarly increased HTLV-1 production in a dose-dependent manner (Fig. 2B).

We next repeated the experiment using MT2 cells instead of 293T cells (Fig. 2C and D). As seen with the 293T cells, BFA or CQ

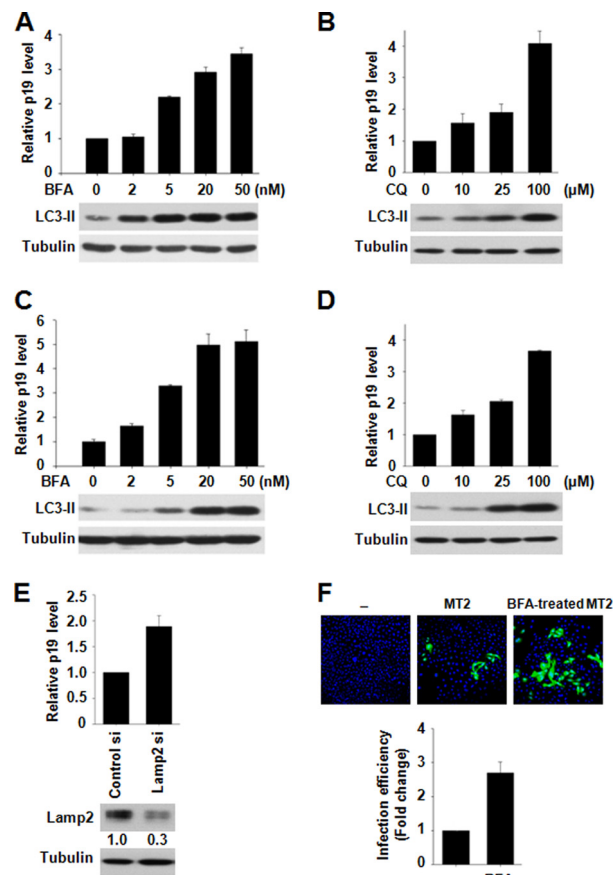


FIG 2 Increased autophagosome accumulation enhanced HTLV-1 production. (A and B) 293T cells were transfected with an HTLV-1 molecular clone (K30) and a Tax-expressing plasmid for 48 h and then treated with the indicated doses of BFA (2 to 50 nM) (A) or CQ (10 to 100 μ M) (B) for 24 h. The amount of HTLV-1 released into the culture supernatants (top, bar graphs) was determined by p19 ELISA according to the manufacturer's instructions. Representative results from three independent experiments are shown as means \pm standard deviation (SD). The cell lysates were Western blotted with anti-LC3B (LC3-II; 14 kDa) and antitubulin (Tubulin) antibodies (bottom, Western blot panels). Tubulin was used as a loading control. (C and D) MT2 cells were treated with the indicated doses of BFA (2 to 50 nM) (C) or CQ (10 to 100 μ M) (D) for 24 h. The release of HTLV-1 into the culture supernatant was determined by p19 ELISA (top, bar graphs). Representative results from three independent experiments are shown as means \pm SD. The cell lysates were Western blotted with anti-LC3B and antitubulin antibodies (bottom, Western blot panels). Tubulin was used as a loading control. (E) MT2 cells were transfected with control siRNA or Lamp2-siRNA for 2 days and then incubated in fresh medium for another 1 day. The release of HTLV-1 into the culture supernatant from these treated MT2 cells was determined by p19 ELISA (top, bar graph). Representative results from three independent experiments are shown as means \pm SD with the value of the control siRNA-treated (si) cells arbitrarily set as 1. The cell lysates were Western blotted with anti-Lamp2 (Lamp2) to verify the efficiency of Lamp2 siRNA-mediated knockdown (bottom, Western blot panels); antitubulin antibody was used to quantify tubulin, which was used as a loading control. The ratios of Lamp2 band intensities were quantified and are enumerated below the top panel. (F) HeLa cells containing an integrated HTLV-1 LTR-GFP reporter were cocultured without MT2 cells (–; top, left) or with MT2 cells (MT2; top, middle) or with MT2 cells pretreated with BFA for 4 h (BFA-treated MT2; top, right) for 3 days. HTLV-1 infection of the HeLa LTR-GFP cells turns the cells green. The infection efficiency was based on counting the number of green cells (HTLV-1-infected cells) per 300 Hoechst dye-stained cells (total cells), arbitrarily setting the value of BFA-untreated MT2 cells as 1 and then calculating the value of BFA-treated MT2 as the fold increase relative to 1. For the bar graph, the average results \pm SD from three independent experiments are shown (bottom, graphs).

treatment of MT2 cells for 24 h significantly increased LC3-II protein levels (Fig. 2C and D, bottom), and we also observed that HTLV-1 production from MT2 cells was increased by BFA and CQ treatments (Fig. 2C and D, bar graphs, top). Thus, these MT2 results (Fig. 2C and D) are in agreement with the 293T findings (Fig. 2A and B). We additionally verified the BFA and CQ results by knockdown of an essential lysosome constituent protein, Lamp2, which is known to produce autophagosome accumulation (60). Lamp2-specific siRNA indeed efficiently knocked down the expression of Lamp2 in MT2 cells by 70% (Fig. 2E, bottom), and this knockdown significantly increased HTLV-1 production, as measured by p19 ELISA (Fig. 2E, bar graph, top). To verify that the released p19 represents infectious virus, we checked the infectivity of untreated MT2 and BFA-treated MT2 using a HeLa-LTR-GFP reporter cell line (Fig. 2F). Using equal numbers of MT2 cells, we found that BFA treatment indeed increased the production of infectious HTLV-1 by approximately 3-fold (Fig. 2F).

Expression of HTLV-1 Tax protein increased autophagosome accumulation. The HTLV-1 Tax protein increases cellular proliferation (55, 61), inhibits apoptosis (62), impairs cell cycle checkpoints (62, 63), and induces DNA damage (64–68). We wondered whether Tax also contributes to HTLV-1-induced autophagosome accumulation (Fig. 1 and 2). Accordingly, we cotransfected HeLa (Fig. 3A) and Jurkat (Fig. 3B) cells with a GFP-Tax plasmid plus a Cherry-LC3 plasmid (Fig. 3A and B; GFP-Tax). Green fluorescence would mark Tax-transfected cells, while the Cherry fluorescence would mark intracellular autophagosomes. As controls, parallel cell cultures were transfected with Cherry-LC3 plasmid plus either an empty vector (Fig. 3A and B; Vector) or a plasmid expressing GFP alone (Fig. 3A and B; GFP). We visualized transfected cells by confocal microscopy and quantified the number of LC3 puncta in cells as a measure of autophagosomes. We observed that the number of Cherry-LC3⁺ puncta (Fig. 3A and B; Cherry) in GFP-Tax-expressing “green” cells was higher by approximately 4-fold than that in cells transfected with empty vector or plasmid expressing GFP alone (Fig. 3A and B, compare GFP-Tax to GFP and Vector). Next, the effect of Tax on the amount of cell endogenous LC3-II protein was quantified by Western blotting. Indeed, in HeLa (Fig. 3C) and Jurkat (Fig. 3D) cells, Tax expression reproducibly increased, in a dose-dependent manner, LC3-II protein levels in cells. Separately, we found that Tax expression did not increase the amount of LC3 mRNA (data not shown), indicating that the observed effects on LC3-II protein occur at a posttranscriptional step.

Tax expression inhibited lysosomal degradation of autophagosomes. The accumulation of autophagosomes in cells can arise from an increase in autophagosome formation or a decrease in autophagosome degradation by lysosomes. To clarify which of these two mechanisms is influenced by Tax, we employed an RFP-GFP-LC3 reporter that expresses a single RFP and GFP doubly in-frame LC3 fusion protein. Thus, the RFP-GFP-LC3 reporter expresses in frame a single fused protein that has the three RFP, GFP, and LC3 open reading frames. Indeed, this expression vector has been used previously to study the autophagosome-to-lysosome fusion step of autophagy (52, 53). The principle underlying this experimental approach is based on the fact that GFP fluorescence is sensitive to the acidic pH of lysosomes, while RFP fluorescence is not. Therefore, the GFP, but not RFP, fluorescent emission produced by the RFP-GFP-LC3 fusion protein is quenched when an RFP-GFP-LC3-expressing autophagosome

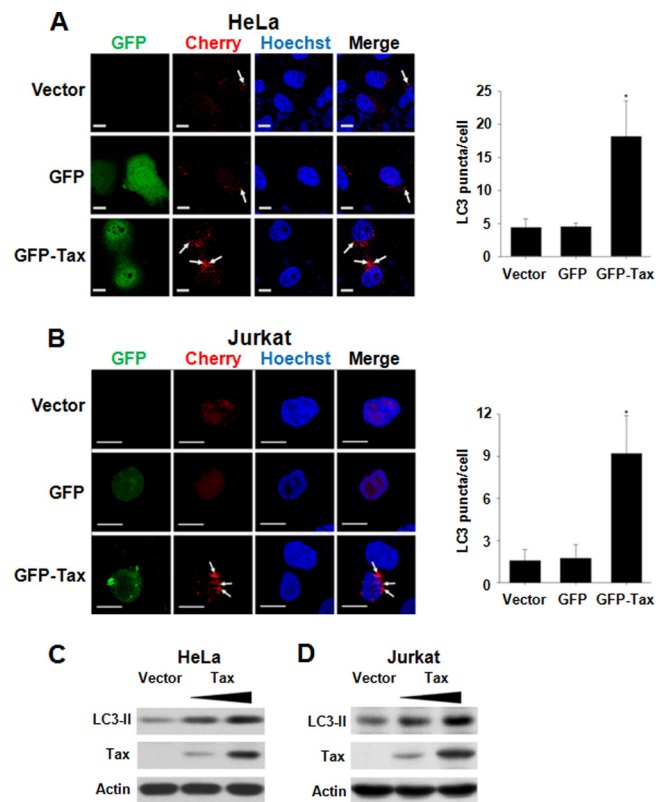


FIG 3 Tax expression increased autophagosome accumulation. HeLa (A) or Jurkat (B) cells were transfected with Cherry-LC3 plasmid plus an empty control vector plasmid (Vector; top row) or Cherry-LC3 plus a GFP-expressing plasmid (GFP; middle row), or Cherry-LC3 plus a GFP-Tax-expressing plasmid (GFP-Tax; bottom row) for 24 h. Cells were visualized for fluorescent signals by confocal microscopy (top). The number of Cherry-LC3 puncta (see arrows) was quantified by visual counting of more than 100 cells. Representative average results from three independent experiments are shown (bar graphs) as means \pm SD. *, $P < 0.05$ by t test. Bars, 10 μ m. HeLa (C) or Jurkat (D) cells were transfected with control vector (Vector) or a Tax-expressing plasmid (Tax) for 24 h, and the cells were harvested and lysed. The lysates were Western blotted with anti-LC3B (LC3-II; 14 kDa), anti-Tax (Tax), or antiactin (Actin) antibodies.

fuses with a lysosome. Under such a circumstance, the autophagosome-lysosome fused organelle would show as an RFP-GFP-LC3 punctum that is RFP driven “red” but without its GFP fluorescence, which is quenched by the acidic milieu. In contrast, if the fusion of an RFP-GFP-LC3-autophagosome with a lysosome is interrupted, then the unfused RFP-GFP-LC3-autophagosome will remain as a punctum that emits both active GFP and the RFP signals (i.e., green plus red). In this case, the integrated green and red fluorescent signals would show as visibly merged yellow fluorescence.

We transfected HeLa cells with the RFP-GFP-LC3 reporter plus either an empty vector plasmid or a Tax-expressing plasmid (Fig. 4) and visualized RFP-GFP-LC3-labeled puncta in these cells. HeLa cells transfected with the RFP-GFP-LC3 reporter plus an empty vector plasmid are expected to go through the normal autophagy process of autophagosome fusion to lysosome. Indeed, in these cells, RFP-GFP-LC3-derived small red puncta (indicative of RFP-positive and GFP-negative emission) were seen in the “merge” window, a finding consistent with the normal process of

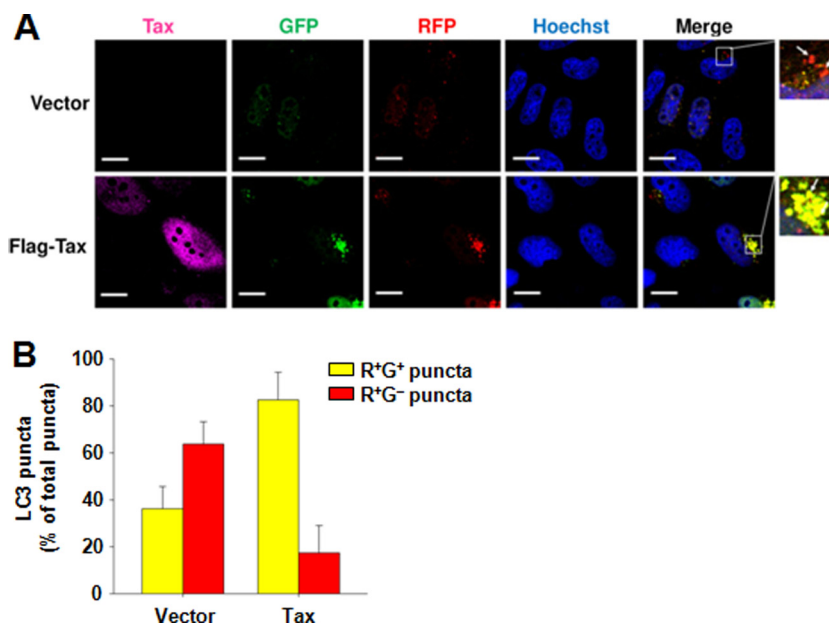


FIG 4 Tax interrupts autophagosome-lysosome fusion. (A) HeLa cells were transfected with RFP-GFP-LC3 plasmid and either an empty control vector plasmid (Vector; top row) or a Flag-Tax-expressing plasmid (Tax; bottom row) for 24 h. The Flag-Tax protein was stained with mouse anti-Flag and anti-mouse secondary antibody labeled with Alexa 647 dye. Fluorescent signals were visualized by confocal microscopy. Pink fluorescence, Tax staining; green fluorescence, GFP; red fluorescence, RFP; blue fluorescence, nuclear staining. Bars, 10 μ m. Shown to the right are enlargements of the areas boxed in the “Merge” panels. (B) The numbers of red-positive and green-positive puncta (R^+G^+) and red-positive and green-negative puncta (R^+G^-) were quantified in more than 50 cells per experiment. The percentages of R^+G^+ puncta and R^+G^- puncta were determined by dividing the number of R^+G^+ puncta or R^+G^- puncta by the total numbers of red or green puncta. Representative average results from three independent experiments are shown as the means \pm SD.

autophagosome-lysosome fusion with acidic quenching of GFP (Fig. 4A, top row; Vector). On the other hand, in HeLa cells transfected with RFP-GFP-LC3 reporter plus Flag-Tax, as expected, the Tax protein induced strong accumulation of RFP-GFP-LC3-puncta (Fig. 4A; see GFP or RFP column). These puncta emit both “red” and “green” fluorescence (R^+/G^+) that is seen as “merged” yellow puncta (Fig. 4A, bottom row; Merge), which is consistent with a lack of acidic quenching of GFP and is indicative of the absence of autophagosome-lysosome fusion. The number of yellow puncta (R^+/G^+) in Tax-expressing cells was significantly increased compared to the number of yellow puncta in control cells (Fig. 4B). Taken together, the findings indicate that Tax expression interrupts autophagy at the step of autophagosome-lysosome fusion. This fusion step is a normal process by which lysosomes degrade autophagosomes. By interrupting this degradation, Tax accordingly increases autophagosome accumulation (Fig. 3).

A Tax mutant incapable of NF- κ B activation failed to enhance autophagosome accumulation. HTLV-1 Tax primarily signals through two major cellular pathways, CREB/ATF and NF- κ B (69). We are interested in understanding how Tax’s signaling activity influences its effect on autophagosome accumulation. To investigate this question, we transfected HeLa cells with wild-type Tax, the Tax M22 mutant (NF- κ B inactive, CREB active), or the Tax M47 mutant (NF- κ B active, CREB inactive) (54) plus a Cherry-LC3 plasmid, and we visualized by confocal microscopy and counted the number of Cherry-LC3-marked puncta in the transfected cells. In these cells, we saw that wild-type Tax and Tax M47 both increased autophagosome accumulation. In contrast, Tax M22 did not (Fig. 5A). We also checked the effects of Tax, Tax M22, and Tax M47 on LC3-II protein levels by Western blotting. Tax and the Tax M47 mutant increased the amount of LC3-II

protein, but Tax M22 did not (LC3-II in Fig. 5B). Additionally, a Tax V89A mutant that is NF- κ B active and CBP/p300 binding defective also increased LC3-II protein levels by Western blotting (see Fig. S1 in the supplemental material). Collectively, these results indicate that Tax activation of the NF- κ B, but not the CREB, pathway is required for increasing autophagosome accumulation.

Autophagosome-lysosome fusion modulates Tax degradation. Autophagosomes are found in the cytoplasm. Several cytoplasmic RNA viruses use these double-membrane vesicles for their genome replication (35, 70). For a nuclear retrovirus such as HTLV-1, it is unclear how inhibition of autophagosome-lysosome fusion by treatment with BFA increases virus production (Fig. 2). Because autophagy is a protein degradation process, it is possible that HTLV-1 proteins like Tax are in part regulated through autophagic degradation. To explore this possibility, we used HTLV-1-infected MT2 cells to ask if the stability of Tax is affected in these cells by BFA treatment. When MT2 cells were treated with BFA for 8 h and 24 h, we observed that the level of Tax protein increased by up to 2-fold after 8 h of treatment (Fig. 6A, compare lane 3 to lane 1) and then up to 3.5-fold at 24 h of treatment (Fig. 6B, compare lane 8 to lane 6). In contrast, treatment of MT2 cells with the proteasome inhibitor MG132 insignificantly changed Tax amounts at the early 8-h time point (Fig. 6A; compare lane 5 to lane 1); however, proteasome inhibition did increase Tax stability by 24 h of treatment (Fig. 6B; compare lane 10 to lane 6). These results suggest that the autophagy and the proteasomal pathways both contribute to Tax degradation, but the former contributes an early component to regulating Tax stability. The findings further suggest that Tax interruption of autophagosome-lysosome fusion (Fig. 4) represents a positive-feedback mechanism on its own stability. In the same vein, interruption by BFA of

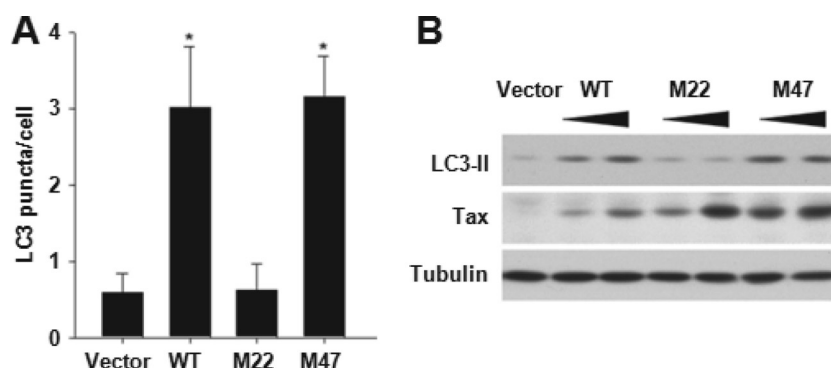


FIG 5 Wild-type Tax and the Tax M47 mutant, but not the Tax M22 mutant, increased autophagosome accumulation. (A) HeLa cells were transfected with the Cherry-LC3 plasmid plus empty vector (Vector) or Cherry-LC3 plus wild-type Tax (WT), or Cherry-LC3 plus the Tax M22 mutant (M22), or Cherry-LC3 plus the Tax M47 mutant (M47) for 24 h. Cells were visualized by confocal microscopy, and the number of Cherry-LC3 puncta was quantified by visual counting of more than 100 cells. Representative average results from three independent experiments are shown as means \pm SD. *, $P < 0.05$ by t test. (B) HeLa cells were transfected with empty vector (Vector) or the wild-type Tax (WT)-, Tax M22 mutant (M22)-, or Tax M47 mutant (M47)-expressing plasmid for 24 h. The cells were then lysed, and the lysates were Western blotted with anti-LC3B (LC3-II; 14 kDa), anti-Tax (Tax), and antitubulin (Tubulin) antibodies.

autophagosome-lysosome fusion could similarly increase Tax stability, which would explain how BFA treatment increases HTLV-1 p19 production in the cell culture supernatant (Fig. 2).

DISCUSSION

Here, we report for the first time that HTLV-1 infection increases autophagosome accumulation in cells in a manner that enhances virus production. We also show that expression of the viral Tax protein acts on autophagosome accumulation by blocking autophagosome-lysosome fusion. Based on results from the mutants Tax M22, M47 (Fig. 5), and V89A which is defective for p300/CBP binding (71) (see Fig. S1 in the supplemental material), we concluded that Tax's ability to activate NF- κ B, but not CREB and p300/CBP, is required for its autophagosome-lysosome blocking activity. Interestingly, it was recently suggested in a review that Tax could activate autophagy through the NF- κ B pathway (48),

and after our manuscript was submitted for publication, a report was published that shows HTLV-2 Tax protein is also able to induce autophagosome accumulation (49). Thus, the effect of Tax on autophagy apparently is conserved between HTLV-1 and HTLV-2.

NF- κ B regulates the expression of various genes involved in cellular proliferation, differentiation, and development, and it is essential for the survival of HTLV-1-infected cells (25, 72, 73). Tax has been found to activate NF- κ B through canonical and noncanonical pathways (25, 72, 73). NF- κ B activation is also known to regulate autophagy in cells through several NF- κ B-responsive downstream autophagy factors that play roles in cell survival under stress conditions (74). Altogether, these findings are consistent with the notion that Tax-NF- κ B activation is important for promoting the survival and proliferation of HTLV-1-infected cells (25, 72, 73). Conversely, the autophagy pathway has been shown to regulate NF- κ B through autophagic degradation of NF- κ B's I κ B kinase (IKK) signaling components (74). Accordingly, the finding here that Tax can block autophagy-mediated protein degradation offers another potential explanation for Tax-NF- κ B activation. Interestingly, by blocking autophagosome-lysosome fusion, Tax appears to moderate its own degradation (Fig. 6) and concordantly may also increase NF- κ B activity. As noted earlier, an increase in Tax protein stability as a result of reduced autophagosome-lysosome fusion can also explain how BFA treatment increases HTLV-1 virus production (Fig. 2). Going forward, determination of the Tax- and/or NF- κ B-responsive factors that are the direct effectors responsible for interrupting autophagosome-lysosome fusion merits thoughtful investigation.

Autophagy is also considered an ancient and highly conserved cellular defense process for lysosomal degradation of invading microbial pathogens (34). Compatible with this view, it has been reported that vesicular stomatitis virus (VSV) infection is suppressed through autophagy induction, and inhibition of autophagy increases its infection (75). Not surprisingly, many viruses have evolved adaptive mechanisms that quell or co-opt the cell's autophagic defense to benefit viral replication. Thus, the HSV-1 ICP34.5 protein and the human herpesvirus 8 (HHV-8) vBCL-2 protein inhibit cellular autophagy through interaction with the cell's Beclin-1 protein (36), and several RNA viruses, such

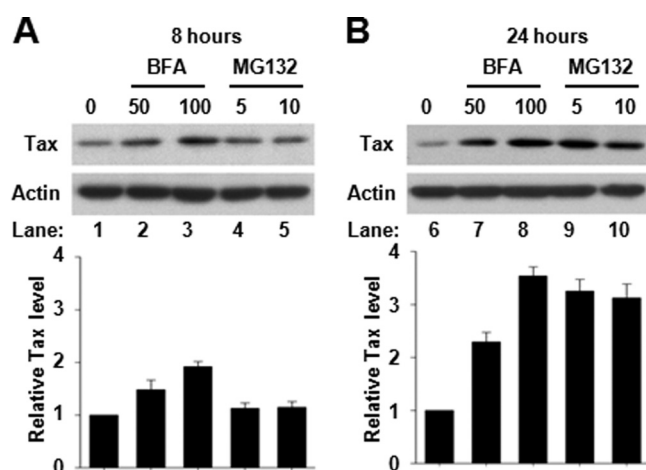


FIG 6 Inhibition of autophagic degradation stabilized the Tax protein level. MT2 cells were treated with BFA (50 or 100 nM) or MG132 (5 or 10 μ M) for 8 h (A) or 24 h (B), and the lysates were Western blotted with anti-Tax and antiactin antibodies (same loadings run on different gels and then blotted). The ratios of band intensities between untreated and drug-treated cells were calculated after normalization to actin. The averages from three independent Western blots are shown (bottom, graphs) as means \pm SD.

as poliovirus and dengue virus, utilize autophagosome membranes to replicate their genomic RNAs (35). The replication of HIV-1, hepatitis C virus (HCV), and hepatitis B virus (HBV) also appears to benefit from autophagosome accumulation, although detailed mechanistic understanding that explains these findings remains to be clarified (35). Our work here adds HTLV-1 to the list of viruses that apparently have evolved capabilities to adapt the cell's autophagic defense into a process that benefits viral replication. The unexpected finding of antiautophagic degradation activity of Tax reflects yet another new facet of the versatile functions of this viral protein in HTLV-1 replication.

To date, many small molecules have been identified as autophagy regulators. Three types of autophagy modulators have been characterized, and some of them are now being used in clinical trials for enhancement of the chemosensitivity of cancers (76, 77). In one group are drugs that suppress autophagy initiation, such as 3-methyladenine and wortmannin (76). These molecules work powerfully, but they have many pleiotropic and off-target activities (78). In another group are molecules that act to disrupt autophagosome degradation by the lysosome; these include BFA and hydroxychloroquine (78, 79). In a final group are autophagy inducers, such as rapamycin, to which have been attributed therapeutic potential for gliomas and advanced renal carcinoma (79) and which have been shown to promote the clearance of protein aggregates in neurodegenerative diseases (80, 81). To our knowledge, no autophagy-related drugs have been employed yet for ATL therapy. The findings here broach, for the first time, the notion that HTLV-1 interacts with the cellular autophagy pathway and raise the consideration that small molecule autophagy regulators could have future uses in the treatment of ATL and other HTLV diseases.

ACKNOWLEDGMENTS

This work was supported through NIAID intramural research funds.

We thank members of the Jeang laboratory for critical reading of the manuscript.

REFERENCES

- Gallo RC. 2005. The discovery of the first human retrovirus: HTLV-1 and HTLV-2. *Retrovirology* 2:17. doi:10.1186/1742-4690-2-17.
- Takatsuki K. 2005. Discovery of adult T-cell leukemia. *Retrovirology* 2:16. doi:10.1186/1742-4690-2-16.
- Martin F, Bangham CR, Ciminale V, Lairmore MD, Murphy EL, Switzer WM, Mahieux R. 2011. Conference highlights of the 15th International Conference on Human Retrovirology: HTLV and related retroviruses, 4–8 June 2011, Leuven, Gembloux, Belgium. *Retrovirology* 8:86. doi:10.1186/1742-4690-8-86.
- Proietti FA, Carneiro-Proietti AB, Catalan-Soares BC, Murphy EL. 2005. Global epidemiology of HTLV-I infection and associated diseases. *Oncogene* 24:6058–6068.
- Ghez D, Lepelletier Y, Jones KS, Pique C, Hermine O. 2010. Current concepts regarding the HTLV-1 receptor complex. *Retrovirology* 7:99. doi:10.1186/1742-4690-7-99.
- Yasunaga J, Matsuoka M. 2011. Molecular mechanisms of HTLV-1 infection and pathogenesis. *Int. J. Hematol.* 94:435–442.
- Gallo RC. 2011. Research and discovery of the first human cancer virus, HTLV-1. *Best Pract. Res. Clin. Haematol.* 24:559–565.
- Yamaguchi K. 1994. Human T-lymphotropic virus type I in Japan. *Lancet* 343:213–216.
- Yoshida M. 2005. Discovery of HTLV-1, the first human retrovirus, its unique regulatory mechanisms, and insights into pathogenesis. *Oncogene* 24:5931–5937.
- Gessain A. 1996. Virological aspects of tropical spastic paraparesis/HTLV-I associated myelopathy and HTLV-I infection. *J. Neurovirol.* 2:299–306.
- Osame M. 2002. Pathological mechanisms of human T-cell lymphotropic virus type I-associated myelopathy (HAM/TSP). *J. Neurovirol.* 8:359–364.
- Giam CZ, Jeang KT. 2007. HTLV-1 Tax and adult T-cell leukemia. *Front. Biosci.* 12:1496–1507.
- Higuchi M, Fujii M. 2009. Distinct functions of HTLV-1 Tax1 from HTLV-2 Tax2 contribute key roles to viral pathogenesis. *Retrovirology* 6:117. doi:10.1186/1742-4690-6-117.
- Robek MD, Ratner L. 1999. immortalization of CD4(+) and CD8(+) T lymphocytes by human T-cell leukemia virus type 1 Tax mutants expressed in a functional molecular clone. *J. Virol.* 73:4856–4865.
- Rosin O, Koch C, Schmitt I, Semmes OJ, Jeang KT, Grassmann R. 1998. A human T-cell leukemia virus Tax variant incapable of activating NF-kappaB retains its immortalizing potential for primary T-lymphocytes. *J. Biol. Chem.* 273:6698–6703.
- Adya N, Zhao LJ, Huang W, Boros I, Giam CZ. 1994. Expansion of CREB's DNA recognition specificity by Tax results from interaction with Ala-Ala-Arg at positions 282–284 near the conserved DNA-binding domain of CREB. *Proc. Natl. Acad. Sci. U. S. A.* 91:5642–5646.
- Green PL, Chen IS. 1990. Regulation of human T cell leukemia virus expression. *FASEB J.* 4:169–175.
- Jeang KT, Boros I, Brady J, Radonovich M, Khoury G. 1988. Characterization of cellular factors that interact with the human T-cell leukemia virus type I p40x-responsive 21-base-pair sequence. *J. Virol.* 62:4499–4509.
- Kim YM, Geiger TR, Egan DI, Sharma N, Nyborg JK. 2010. The HTLV-1 tax protein cooperates with phosphorylated CREB, TORC2 and p300 to activate CRE-dependent cyclin D1 transcription. *Oncogene* 29:2142–2152.
- Kwok RP, Laurance ME, Lundblad JR, Goldman PS, Shih H, Connor LM, Marriott SJ, Goodman RH. 1996. Control of cAMP-regulated enhancers by the viral transactivator Tax through CREB and the co-activator CBP. *Nature* 380:642–646.
- Siu YT, Chin KT, Siu KL, Yee Wai Choy E, Jeang KT, Jin DY. 2006. TORC1 and TORC2 coactivators are required for tax activation of the human T-cell leukemia virus type 1 long terminal repeats. *J. Virol.* 80:7052–7059.
- Bonnet A, Randrianarison-Huetz V, Nzounza P, Nedelec M, Chazal M, Waast L, Pene S, Bazarbachi A, Mahieux R, Benit L, Pique C. 2012. Low nuclear body formation and tax SUMOylation do not prevent NF-kappaB promoter activation. *Retrovirology* 9:77. doi:10.1186/1742-4690-9-77.
- Boxus M, Twizere JC, Legros S, Dewulf JF, Kettmann R, Willems L. 2008. The HTLV-1 Tax interactome. *Retrovirology* 5:76. doi:10.1186/1742-4690-5-76.
- Ng PW, Iha H, Iwanaga Y, Bittner M, Chen Y, Jiang Y, Gooden G, Trent JM, Meltzer P, Jeang KT, Zeichner SL. 2001. Genome-wide expression changes induced by HTLV-1 Tax: evidence for MLK-3 mixed lineage kinase involvement in Tax-mediated NF-kappaB activation. *Oncogene* 20:4484–4496.
- Peloponese JM, Yeung ML, Jeang KT. 2006. Modulation of nuclear factor-kappaB by human T cell leukemia virus type 1 Tax protein: implications for oncogenesis and inflammation. *Immunol. Res.* 34:1–12.
- Simonis N, Rual JF, Lemmens I, Boxus M, Hirozane-Kishikawa T, Gatot JS, Dricot A, Hao T, Vertommen D, Legros S, Daakour S, Klitgord N, Martin M, Willaert JF, Dequiedt F, Navratil V, Cusick ME, Burny A, Van Lint C, Hill DE, Tavernier J, Kettmann R, Vidal M, Twizere JC. 2012. Host-pathogen interactome mapping for HTLV-1 and -2 retroviruses. *Retrovirology* 9:26. doi:10.1186/1742-4690-9-26.
- Xiao G. 2012. NF-kappaB activation: Tax sumoylation is out, but what about Tax ubiquitination? *Retrovirology* 9:78. doi:10.1186/1742-4690-9-78.
- Glick D, Barth S, Macleod KF. 2010. Autophagy: cellular and molecular mechanisms. *J. Pathol.* 221:3–12.
- Xie Z, Klionsky DJ. 2007. Autophagosome formation: core machinery and adaptations. *Nat. Cell Biol.* 9:1102–1109.
- Klionsky DJ, Abeliovich H, Agostinis P, Agrawal DK, Aliev G, Askew DS, Baba M, Baehrecke EH, Bahr BA, Ballabio A, Bamber BA, Bassham DC, Bergamini E, Bi X, Biard-Piechaczyk M, Blum JS, Bredeken DE, Brodsky JL, Brumell JH, Brunk UT, Bursch W, Camougrand N, Cebollero E, Cecconi F, Chen Y, Chin LS, Choi A, Chu CT, Chung J, Clarke PG, Clark RS, Clarke SG, Clave C, Cleveland JL, Codogno P, Colombo MI, Coto-Montes A, Cregg JM, Cuervo AM, Debnath J, Demarchi F, Dennis PB, Dennis PA, Deretic V, Devenish RJ, Di Sano F, Dice JF, Difiglia M, Dinesh-Kumar S, Distelhorst CW, Djavaheri-

- Mergny M, Dorsey FC, Droge W, Dron M, Dunn WA, Jr, Duszenko M, Eissa NT, Elazar Z, Esclatine A, Eskelinen EL, Fesus L, Finley KD, Fuentes JM, Fueyo J, Fujisaki K, Galliot B, Gao FB, Gewirtz DA, Gibson SB, Gohla A, Goldberg AL, Gonzalez R, Gonzalez-Estevez C, Gorski S, Gottlieb RA, Haussinger D, He YW, Heidenreich K, Hill JA, Hoyer-Hansen M, Hu X, Huang WP, Iwasaki A, Jaattela M, Jackson WT, Jiang X, Jin S, Johansen T, Jung JU, Kadowaki M, Kang C, Kelekar A, Kessel DH, Kiel JA, Kim HP, Kimchi A, Kinsella TJ, Kiselyov K, Kitamoto K, Knecht E, et al. 2008. Guidelines for the use and interpretation of assays for monitoring autophagy in higher eukaryotes. *Autophagy* 4:151–175.
31. Knaevelsrud H, Simonsen A. 2012. Lipids in autophagy: constituents, signaling molecules and cargo with relevance to disease. *Biochim. Biophys. Acta* 1821:1133–1145.
32. Levine B, Kroemer G. 2008. Autophagy in the pathogenesis of disease. *Cell* 132:27–42.
33. Dreux M, Chisari FV. 2010. Viruses and the autophagy machinery. *Cell Cycle* 9:1295–1307.
34. Tang SW, Ducroux A, Jeang KT, Neuveut C. 2012. Impact of cellular autophagy on viruses: insights from hepatitis B virus and human retroviruses. *J. Biomed. Sci.* 19:92. doi:10.1186/1423-0127-19-92.
35. Sir D, Ou JH. 2010. Autophagy in viral replication and pathogenesis. *Mol. Cells* 29:1–7.
36. Cavnac Y, Esclatine A. 2010. Herpesviruses and autophagy: catch me if you can! *Viruses* 2:314–333.
37. English L, Chemali M, Duron J, Rondeau C, Laplante A, Gingras D, Alexander D, Leib D, Norbury C, Lippe R, Desjardins M. 2009. Autophagy enhances the presentation of endogenous viral antigens on MHC class I molecules during HSV-1 infection. *Nat. Immunol.* 10:480–487.
38. Gannage M, Dormann D, Albrecht R, Dengjel J, Torossi T, Ramer PC, Lee M, Strowitz T, Arrey F, Conenello G, Pypaert M, Andersen J, Garcia-Sastre A, Munz C. 2009. Matrix protein 2 of influenza A virus blocks autophagosome fusion with lysosomes. *Cell Host Microbe* 6:367–380.
39. Borel S, Espert L, Biard-Piechaczyk M. 2012. Macroautophagy regulation during HIV-1 infection of CD4+ T cells and macrophages. *Front. Immunol.* 3:97. doi:10.3389/fimmu.2012.00097.
40. Espert L, Varbanov M, Robert-Hebmann V, Sagnier S, Robbins I, Sanchez F, Lafont V, Biard-Piechaczyk M. 2009. Differential role of autophagy in CD4 T cells and macrophages during X4 and R5 HIV-1 infection. *PLoS One* 4:e5787. doi:10.1371/journal.pone.0005787.
41. Kyei GB, Dinkins C, Davis AS, Roberts E, Singh SB, Dong C, Wu L, Kominami E, Ueno T, Yamamoto A, Federico M, Panganiban A, Vergne I, Deretic V. 2009. Autophagy pathway intersects with HIV-1 biosynthesis and regulates viral yields in macrophages. *J. Cell Biol.* 186:255–268.
42. Wang X, Gao Y, Tan J, Devadas K, Ragupathy V, Takeda K, Zhao J, Hewlett I. 2012. HIV-1 and HIV-2 infections induce autophagy in Jurkat and CD4+ T cells. *Cell. Signal.* 24:1414–1419.
43. Zhou D, Spector SA. 2008. Human immunodeficiency virus type-1 infection inhibits autophagy. *AIDS* 22:695–699.
44. Li JC, Au KY, Fang JW, Yim HC, Chow KH, Ho PL, Lau AS. 2011. HIV-1 trans-activator protein dysregulates IFN-gamma signaling and contributes to the suppression of autophagy induction. *AIDS* 25:15–25.
45. Van Grol J, Subauste C, Andrade RM, Fujinaga K, Nelson J, Subauste CS. 2010. HIV-1 inhibits autophagy in bystander macrophage/monocytic cells through Src-Akt and STAT3. *PLoS One* 5:e11733. doi:10.1371/journal.pone.0011733.
46. Campbell GR, Spector SA. 2011. Hormonally active vitamin D3 (1 α -ph,25-dihydroxycholecalciferol) triggers autophagy in human macrophages that inhibits HIV-1 infection. *J. Biol. Chem.* 286:18890–18902.
47. Campbell GR, Spector SA. 2012. Vitamin D inhibits human immunodeficiency virus type 1 and Mycobacterium tuberculosis infection in macrophages through the induction of autophagy. *PLoS Pathog.* 8:e1002689. doi:10.1371/journal.ppat.1002689.
48. Cheng H, Ren T, Sun SC. 2012. New insight into the oncogenic mechanism of the retroviral oncoprotein Tax. *Protein Cell* 3:581–589.
49. Ren T, Dong W, Takahashi Y, Xiang D, Yuan Y, Liu X, Loughran TP, Jr, Sun SC, Wang HG, Cheng H. 2012. HTLV-2 Tax immortalizes human CD4+ memory T lymphocytes by oncogenic activation and dysregulation of autophagy. *J. Biol. Chem.* 287:34683–34693.
50. Pankiv S, Clausen TH, Lamark T, Brech A, Bruun JA, Outzen H, Overvatn A, Bjorkoy G, Johansen T. 2007. p62/SQSTM1 binds directly to Atg8/LC3 to facilitate degradation of ubiquitinated protein aggregates by autophagy. *J. Biol. Chem.* 282:24131–24145.
51. Zhao TM, Robinson MA, Bowers FS, Kindt TJ. 1995. Characterization of an infectious molecular clone of human T-cell leukemia virus type I. *J. Virol.* 69:2024–2030.
52. Kabeya Y, Mizushima N, Ueno T, Yamamoto A, Kirisako T, Noda T, Kominami E, Ohsumi Y, Yoshimori T. 2000. LC3, a mammalian homologue of yeast Apg8p, is localized in autophagosome membranes after processing. *EMBO J.* 19:5720–5728.
53. Kimura S, Noda T, Yoshimori T. 2007. Dissection of the autophagosome maturation process by a novel reporter protein, tandem fluorescently-tagged LC3. *Autophagy* 3:452–460.
54. Smith MR, Greene WC. 1990. Identification of HTLV-I tax transactivator mutants exhibiting novel transcriptional phenotypes. *Genes Dev.* 4:1875–1885.
55. Zane L, Sibon D, Jeannin L, Zandecki M, Delfau-Larue MH, Gessain A, Gout O, Pinatel C, Lancon A, Mortreux F, Wattel E. 2010. Tax gene expression and cell cycling but not cell death are selected during HTLV-1 infection in vivo. *Retrovirology* 7:17. doi:10.1186/1742-4690-7-17.
56. Chen CY, Chi YH, Mutalif RA, Starost MF, Myers TG, Anderson SA, Stewart CL, Jeang KT. 2012. Accumulation of the inner nuclear envelope protein Sun1 is pathogenic in progeric and dystrophic laminopathies. *Cell* 149:565–577.
57. Yamamoto A, Tagawa Y, Yoshimori T, Moriyama Y, Masaki R, Tashiro Y. 1998. Bafilomycin A1 prevents maturation of autophagic vacuoles by inhibiting fusion between autophagosomes and lysosomes in rat hepatoma cell line, H-4-II-E cells. *Cell Struct. Funct.* 23:33–42.
58. Chen PM, Gombart ZJ, Chen JW. 2011. Chloroquine treatment of ARPE-19 cells leads to lysosome dilation and intracellular lipid accumulation: possible implications of lysosomal dysfunction in macular degeneration. *Cell Biosci.* 1:10. doi:10.1186/2045-3701-1-10.
59. Seglen PO, Grinde B, Solheim AE. 1979. Inhibition of the lysosomal pathway of protein degradation in isolated rat hepatocytes by ammonia, methylamine, chloroquine and leupeptin. *Eur. J. Biochem.* 95:215–225.
60. Tanaka Y, Guhde G, Suter A, Eskelinen EL, Hartmann D, Lullmann-Rauch R, Janssen PM, Blanz J, von Figura K, Saftig P. 2000. Accumulation of autophagic vacuoles and cardiomyopathy in LAMP-2-deficient mice. *Nature* 406:902–906.
61. Boxus M, Twizere JC, Legros S, Kettmann R, Willems L. 2012. Interaction of HTLV-1 Tax with minichromosome maintenance proteins accelerates the replication timing program. *Blood* 119:151–160.
62. Boxus M, Willems L. 2012. How the DNA damage response determines the fate of HTLV-1 Tax-expressing cells. *Retrovirology* 9:2. doi:10.1186/1742-4690-9-2.
63. Peloponese JM, Jr, Haller K, Miyazato A, Jeang KT. 2005. Abnormal centrosome amplification in cells through the targeting of Ran-binding protein-1 by the human T cell leukemia virus type-1 Tax oncoprotein. *Proc. Natl. Acad. Sci. U. S. A.* 102:18974–18979.
64. Belgnaoui SM, Fryrear KA, Nyalwidhe JO, Guo X, Semmes OJ. 2010. The viral oncoprotein tax sequesters DNA damage response factors by tethering MDC1 to chromatin. *J. Biol. Chem.* 285:32897–32905.
65. Gatz ML, Watt JC, Marriott SJ. 2003. Cellular transformation by the HTLV-1 Tax protein, a jack-of-all-trades. *Oncogene* 22:5141–5149.
66. Majone F, Jeang KT. 2000. Clastogenic effect of the human T-cell leukemia virus type I Tax oncoprotein correlates with unstabilized DNA breaks. *J. Biol. Chem.* 275:32906–32910.
67. Majone F, Jeang KT. 2012. Unstabilized DNA breaks in HTLV-1 Tax expressing cells correlate with functional targeting of Ku80, not PKcs, XRCC4, or H2AX. *Cell Biosci.* 2:15. doi:10.1186/2045-3701-2-15.
68. Ramadan E, Ward M, Guo X, Durkin SS, Sawyer A, Vilela M, Osgood C, Pothan A, Semmes OJ. 2008. Physical and in silico approaches identify DNA-PK in a Tax DNA-damage response interactome. *Retrovirology* 5:92. doi:10.1186/1742-4690-5-92.
69. Matsuoka M, Jeang KT. 2011. Human T-cell leukemia virus type 1 (HTLV-1) and leukemic transformation: viral infectivity, Tax, HBZ and therapy. *Oncogene* 30:1379–1389.
70. Jackson WT, Giddings TH, Jr, Taylor MP, Mulinyawe S, Rabinovitch M, Kopito RR, Kirkegaard K. 2005. Subversion of cellular autophagosome machinery by RNA viruses. *PLoS Biol.* 3:e156. doi:10.1371/journal.pbio.0030156.
71. Harrod R, Tang Y, Nicot C, Lu HS, Vassilev A, Nakatani Y, Giam CZ. 1998. An exposed KID-like domain in human T-cell lymphotropic virus type 1 Tax is responsible for the recruitment of coactivators CBP/p300. *Mol. Cell. Biol.* 18:5052–5061.

72. Harhaj EW, Harhaj NS. 2005. Mechanisms of persistent NF-kappaB activation by HTLV-I tax. *IUBMB Life* 57:83–91.
73. Qu Z, Xiao G. 2011. Human T-cell lymphotropic virus: a model of NF-kappaB-associated tumorigenesis. *Viruses* 3:714–749.
74. Trocoli A, Djavaheri-Mergny M. 2011. The complex interplay between autophagy and NF-kappaB signaling pathways in cancer cells. *Am. J. Cancer Res.* 1:629–649.
75. Shelly S, Lukinova N, Bambina S, Berman A, Cherry S. 2009. Autophagy is an essential component of Drosophila immunity against vesicular stomatitis virus. *Immunity* 30:588–598.
76. Chen S, Rehman SK, Zhang W, Wen A, Yao L, Zhang J. 2010. Autophagy is a therapeutic target in anticancer drug resistance. *Biochim. Biophys. Acta* 1806:220–229.
77. Yang ZJ, Chee CE, Huang S, Sinicrope FA. 2011. The role of autophagy in cancer: therapeutic implications. *Mol. Cancer Ther.* 10:1533–1541.
78. Amaravadi RK, Lippincott-Schwartz J, Yin XM, Weiss WA, Takebe N, Timmer W, DiPaola RS, Lotze MT, White E. 2011. Principles and current strategies for targeting autophagy for cancer treatment. *Clin. Cancer Res.* 17:654–666.
79. Rubinsztein DC, Gestwicki JE, Murphy LO, Klionsky DJ. 2007. Potential therapeutic applications of autophagy. *Nat. Rev. Drug Discov.* 6:304–312.
80. Ross CA, Tabrizi SJ. 2011. Huntington's disease: from molecular pathogenesis to clinical treatment. *Lancet Neurol.* 10:83–98.
81. Sarkar S, Perlstein EO, Imarisio S, Pineau S, Cordenier A, Maglathlin RL, Webster JA, Lewis TA, O'Kane CJ, Schreiber SL, Rubinsztein DC. 2007. Small molecules enhance autophagy and reduce toxicity in Huntington's disease models. *Nat. Chem. Biol.* 3:331–338.